Inorg. Chem. **2007**, *46*, 3511–3522

The Origin of the Surprising Stabilities of Highly Charged Self-Assembled Polymetallic Complexes in Solution

Gabriel Canard and Claude Piguet*

Department of Inorganic, Analytical and Applied Chemistry, University of Geneva, 30 quai E. Ansermet, CH-1211 Geneva 4, Switzerland

Received November 9, 2006

The thermodynamics of electrochemical and complexation reactions involving the heterobimetallic triple-stranded helicates $[MA(\mathbf{L5})_3]^{n+}$ (M = Ru(II), Cr(III) and A = Ca(II), Lu(III)) reveal that solvation processes mask intramolecular intermetallic repulsions in solution, a phenomenon at the origin of the surprising stabilities of highly charged self-assembled polymetallic complexes in solution. A judicious combination of Born–Haber cycles and the Born equation restores the expected electrostatic trend in the gas phase, in which intermetallic interactions can be simply modeled using a standard Coulombic approach. Semiquantitative estimation and prediction of the contribution of the intermetallic repulsion to the total free energy of the formation of discrete polymetallic assemblies in solution become thus accessible. This point is crucial for programming stable metallosupramolecular architectures in solution.

Introduction

Although the straightforward application of Coulomb eq 1 predicts a significant intermetallic repulsion $\Delta E^{MM}_{calcd} = W_{elec} = 10.4$ kJ mol^{-1} between two adjacent monocharged cations separated by $d = 5.8$ Å in the double-stranded helicates $[Cu_3(\mathbf{L1})_2]^{3+}$ and $[Ag_3(\mathbf{L2})_2]^{3+}$, which disfavors successive metallic complexation, Lehn and co-workers surprisingly reported that the formation of these trinuclear complexes was driven to completion by positive cooperativity (N_{Av} is Avogadro's number = 6.023×10^{23} mol^{-1}, z_i are the charges of the interacting particles in electrostatic units, e is the elemental charge = 1.602×10^{-19} C, ϵ_0 is the vacuum permittivity constant = 8.859×10^{-12} C N^{-1} m^{-2}, ϵ_r is the relative dielectric permittivity of the medium = 23 in acetonitrile/chloroform, and d is the intermetallic separation).[1,2] A decade later, the thorough investigation of their mechanism of formation[3] combined with a careful re-examination of the thermodynamic modeling of self-assembly processes eventually reached the opposite conclusion that negative cooperativity indeed dominates the complexation events operating in $[Cu_3(\mathbf{L1})_2]^{3+}$ and in$[Ag_3(\mathbf{L2})_2]^{3+}$.[4–6]

$$\Delta E^{MM}_{calcd} = W_{elec} = -\frac{N_{av} z_1 z_2 e^2}{4\pi\epsilon_0}\int_{\infty}^{d}\frac{dr}{\epsilon_r r^2} \qquad (1)$$

However, the best fit of the thermodynamic data leading to $[Cu_3(\mathbf{L1})_2]^{3+}$ in acetonitrile/chloroform displayed an attractive microscopic intermetallic interactions $\Delta E^{CuCu}_{exp,sol} < 0$, a mathematical solution discarded at that time because it was counterintuitive and irrelevant when the expected repulsive electrostatic interaction operating between two cations was modeled.[5b] Although less striking, the fitted value $\Delta E^{EuEu}_{exp,sol} = 14$ kJ mol^{-1} for the intermetallic Eu(III)···Eu(III) interaction, occurring at 9 Å in the polymetallic helicates $[Eu_3(\mathbf{L3})_3]^{9+}$, poorly matches the value, $\Delta E^{EuEu}_{calcd} = 38$ kJ mol^{-1}, computed with eq 1 in a continuous dielectric ($\epsilon_r = 36.1$ for acetonitrile).[5b] Moreover, a reliable prediction of the stability constant for the tetrametallic analogue $[Eu_4(\mathbf{L4})_3]^{12+}$ could be only obtained when $\Delta E^{EuEu}_{exp,sol} = 14$ kJ mol^{-1} is taken into account.[7] This recurrent enigma also

* To whom correspondence should be addressed. E-mail: Claude.Piguet@chiam.unige.ch.

(1) Lehn, J.-M.; Rigault, A.; Siegel, J.; Harrowfield, J.; Chevrier, B.; Moras, D. *Proc. Natl. Acad. Sci. U.S.A.* **1987**, *84*, 2565−2569.
(2) (a) Pfeil, A.; Lehn, J.-M. *J. Chem. Soc., Chem. Commun.* **1992**, 838−840. (b) Garrett, T. M.; Koert, U.; Lehn, J.-M. *J. Phys. Org. Chem.* **1992**, *5*, 529−533.
(3) Fatin-Rouge, N.; Blanc, S.; Pfeil, A.; Rigault, A.; Albrecht-Gary, A.-M.; Lehn, J.-M. *Helv. Chim. Acta* **2001**, *84*, 1694−1711.
(4) Ercolani, G. *J. Am. Chem. Soc.* **2003**, *125*, 16097−16103.
(5) (a) Hamacek, J.; Borkovec, M.; Piguet, C. *Chem.—Eur. J.* **2005**, *11*, 5217−5226. (b) Hamacek, J.; Borkovec, M.; Piguet, C. *Chem.—Eur. J.* **2005**, *11*, 5227−5237.
(6) Hamacek, J.; Piguet, C. *J. Phys. Chem. B* **2006**, *110*, 7783−7792.
(7) Zeckert, K.; Hamacek, J.; Senegas, J.-M.; Dalla-Favera, N.; Floquet, S.; Bernardinelli, G.; Piguet, C. *Angew. Chem., Int. Ed.* **2005**, *44*, 7954−7958.

10.1021/ic062126o CCC: $37.00
Published on Web 04/05/2007

Chart 1

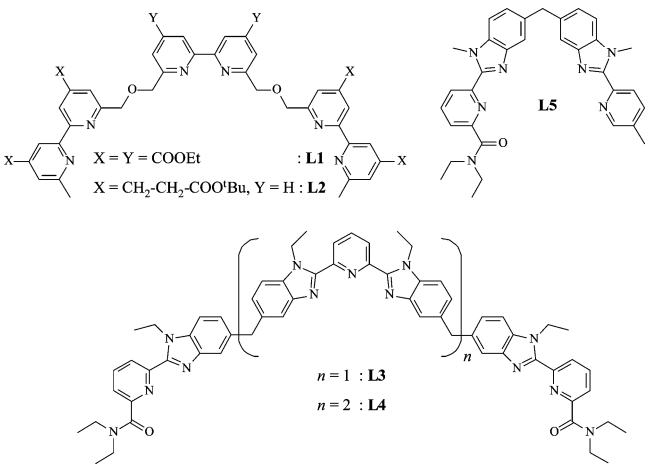

arises when a trivalent lanthanide, Ln(III), coordinates to the inert and facial noncovalent tripods $[Cr(\mathbf{L5})_3]^{3+}$. An experimental electrostatic work of only 9 kJ mol^{-1} is found in acetonitrile for the two triply charged ions at 9.3 Å in $[CrLn(\mathbf{L5})_3]^{6+}$, while eq 1 predicts $W_{elec} = 37$ kJ mol^{-1} ($\epsilon_r = 36.1$, $d_{CrLn} = 9.3$ Å, Figure 1b).[8]To design stable molecular or supramolecular assemblies including charged components, this systematic deviation from a simple electrostatic model, which indeed reduces intramolecular intermetallic repulsion, should be addressed. Three possible origins for the rationalization of these phenomena can be envisioned: (i) the breakdown of the dielectric continuum in molecules, which would require the concept of local dielectric constants,[9] (ii) specific charge compensation effects in the complexes which affect the Coulombic model, and (iii) specific solvation effects. This contribution thus aims to reconcile experimental intermetallic interactions recorded in solution ($\Delta E^{MM}_{exp,sol}$) with a classical Coulombic approach (ΔE^{MM}_{calcd}) derived from eq 1. We focus here on two simple chemical processes, in which the electrostatic contribution to the total free energy change can be easily modeled with eq 1 (Figure 1). First, the Ru(III)/Ru(II)-centered reduction of the triple-stranded helicate $[Ru^{III}A(\mathbf{L5})_3]^{(3+z)+}$ (A = nothing, noted Ø in the rest of the text, $z = 0$; A = Ca(II), $z = 2$; A = Lu(III), $z = 3$) will be considered as a probe for the investigation of a simple charge transfer occurring in the vicinity of a charged but electrochemically inactive spectator cation (A^{z+}, Figure 1a). Second, the complexation process shown in Figure 1b will be compared for two different cationic tripods $[Ru(\mathbf{L5})_3]^{2+}$ and $[Cr(\mathbf{L5})_3]^{3+}$, which differ only in their total charge.

Results and Discussions

Syntheses and Characterization of the Complexes $[Ru(\mathbf{L5})_3](CF_3SO_3)_2$, $[RuCa(\mathbf{L5})_3](CF_3SO_3)_4$, and $[RuLu(\mathbf{L5})_3](CF_3SO_3)_5$. For bimetallic double- or triple-helical complexes involving heterotopic (i.e., unsymmetrical) ligands, two different isomers exist, depending on the relative arrangement

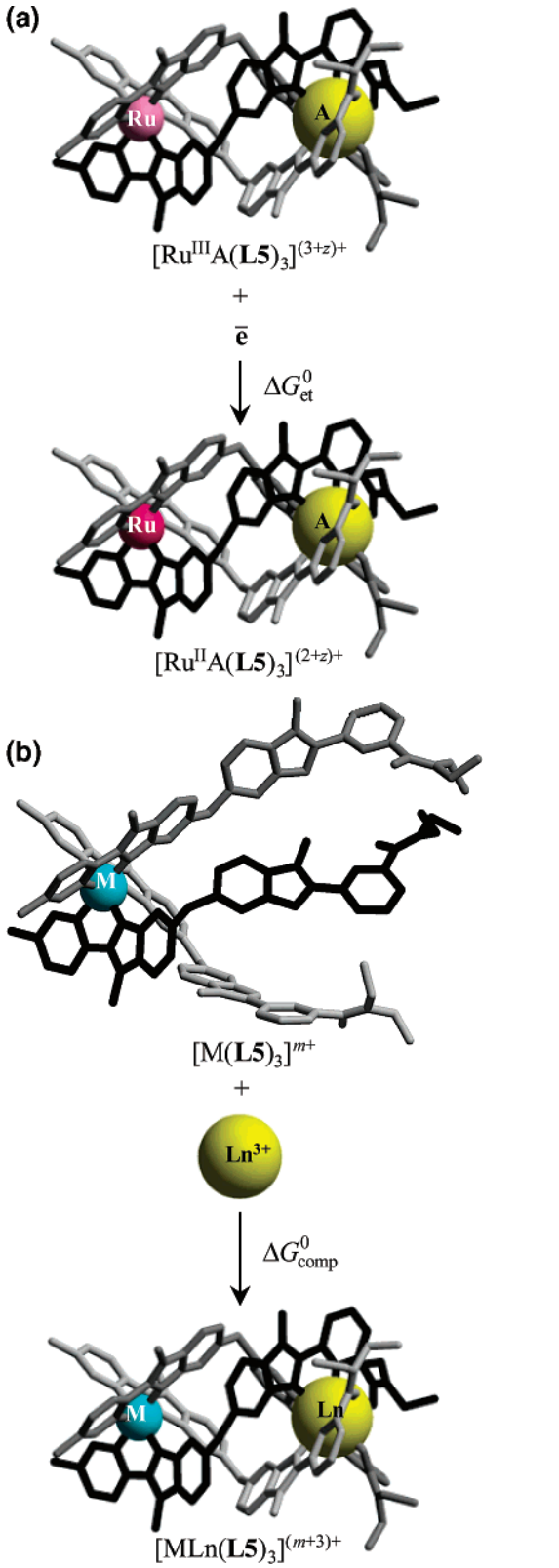

Figure 1. (a) Schematic thermodynamic Ru-centered reduction of the heterobimetallic triple-stranded helicates $[Ru^{III}A(\mathbf{L5})_3]^{(3+z)+}$ (A = Ø, $z = 0$; A = Ca(II), $z = 2$; A = Lu, $z = 3$). (b) Schematic thermodynamic complexation of trivalent lanthanides, Ln(III), to the facial inert noncovalent receptors $[M(\mathbf{L5})_3]^{m+}$ (M = Ru(II), $m = 2$; M = Cr(III), $m = 3$).

of the strands.[10] For $[RuA(\mathbf{L5})_3]^{(2+z)+}$ (A = Ø, $z = 0$; A = Ca(II), $z = 2$; A = Lu(III), $z = 3$), the head-to-head-to-head isomer *HHH*-$[RuA(\mathbf{L5})_3]^{(2+z)+}$ results when the three strands

(8) Cantuel, M.; Bernardinelli, G.; Muller, G.; Riehl, J. P.; Piguet, C. *Inorg. Chem.* **2004**, *43*, 1840−1849.
(9) (a) Richardi, J.; Krienke, H.; Fries, P. H. *Chem. Phys. Lett.* **1997**, *273*, 115−121. (b) Sacco, A.; Belorizky, E.; Jeannin, M.; Gorecki, W.; Fries, P. H. *J. Phys. II Fr.* **1997**, *7*, 1299−1322.

Scheme 1. Syntheses of Complexes *HHH*-[RuA(**L5**)$_3$](CF$_3$SO$_3$)$_{(2+z)}$ (A = Ø, z = 0; A = Ca, z = 2; A = Lu, z = 3) with Numbering Scheme for ^{1}H NMR Experiments

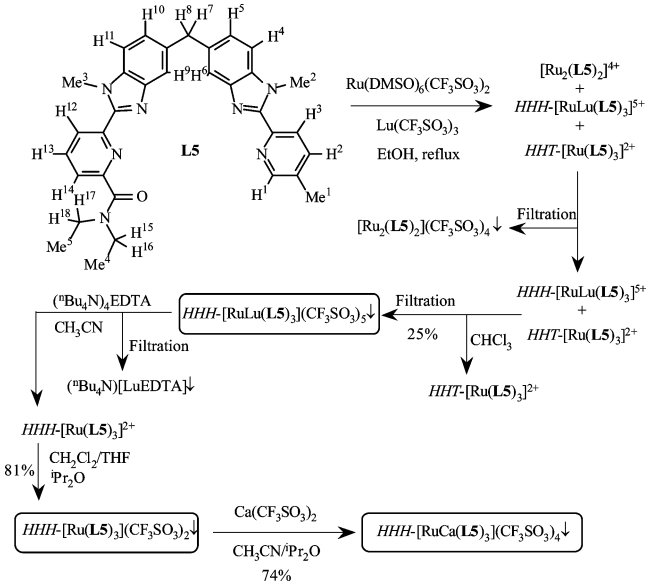

adopt a parallel organization leading to a threefold symmetrical complex, in which Ru(II) is octahedrally coordinated by the three bidentate binding units and A^{z+} is nine-coordinated by the three tridentate binding units, as exemplified in Figure 1. A reverse arrangement of one strand produces the head-to-head-to-tail C_1-symmetrical isomer *HHT*-[RuA(**L5**)$_3$]$^{(2+z)+}$. This rather tedious terminology will be used for the discussion of the synthetic strategy to avoid any confusion. However, for the rest of the manuscript, the notation [RuA(**L5**)$_3$]$^{(2+z)+}$ strictly refers to the axial isomer *HHH*-[RuA(**L5**)$_3$]$^{(2+z)+}$.

Inspired by a previously published procedure,[11] an improved method has been developed for the syntheses of Ru-containing d−f triple-stranded helicates (Scheme 1). *HHH*-[RuLu(**L5**)$_3$]$^{5+}$ is thus obtained in a 25% yield by the reaction of Ru(DMSO)$_6$(CF$_3$SO$_3$)$_2$ (1 equiv), **L5** (3 equiv), and Lu(CF$_3$SO$_3$)$_3$ (1 equiv) in refluxing ethanol, followed by a careful purification process, which aims to remove the large amount of the undesirable *HHT*-[Ru(**L5**)$_3$]$^{2+}$ and [Ru$_2$(**L5**)$_2$]$^{4+}$ side products (Scheme 1 and Figure 2a and b). Upon further treatment of *HHH*-[RuLu(**L5**)$_3$]$^{5+}$ with EDTA^{4-} in acetonitrile, the insoluble lanthanide salt (^{n}Bu$_4$N)Lu(EDTA) is separated by filtration, and the resulting noncovalent tripod *HHH*-[Ru(**L5**)$_3$]$^{2+}$ is crystallized as its trifluoromethanesulfonate salt in an 81% yield (Scheme 1 and Figure 2c).[8,12] Finally, the recombination of *HHH*-[Ru(**L5**)$_3$]$^{2+}$ with Ca(CF$_3$SO$_3$)$_2$ in acetonitrile provides *HHH*-[RuCa(**L5**)$_3$]$^{4+}$ in a 74% yield (Scheme 1). It is worth noting that *HHH*-[RuCa(**L5**)$_3$]$^{4+}$ cannot be obtained directly by the reaction of Ru(DMSO)$_6$(CF$_3$SO$_3$)$_2$ (1 equiv), **L5** (3 equiv), and Ca(CF$_3$SO$_3$)$_2$ (1 equiv), which suggests that, despite the modest overall yield (25%), the templating effect of Lu(III) in the

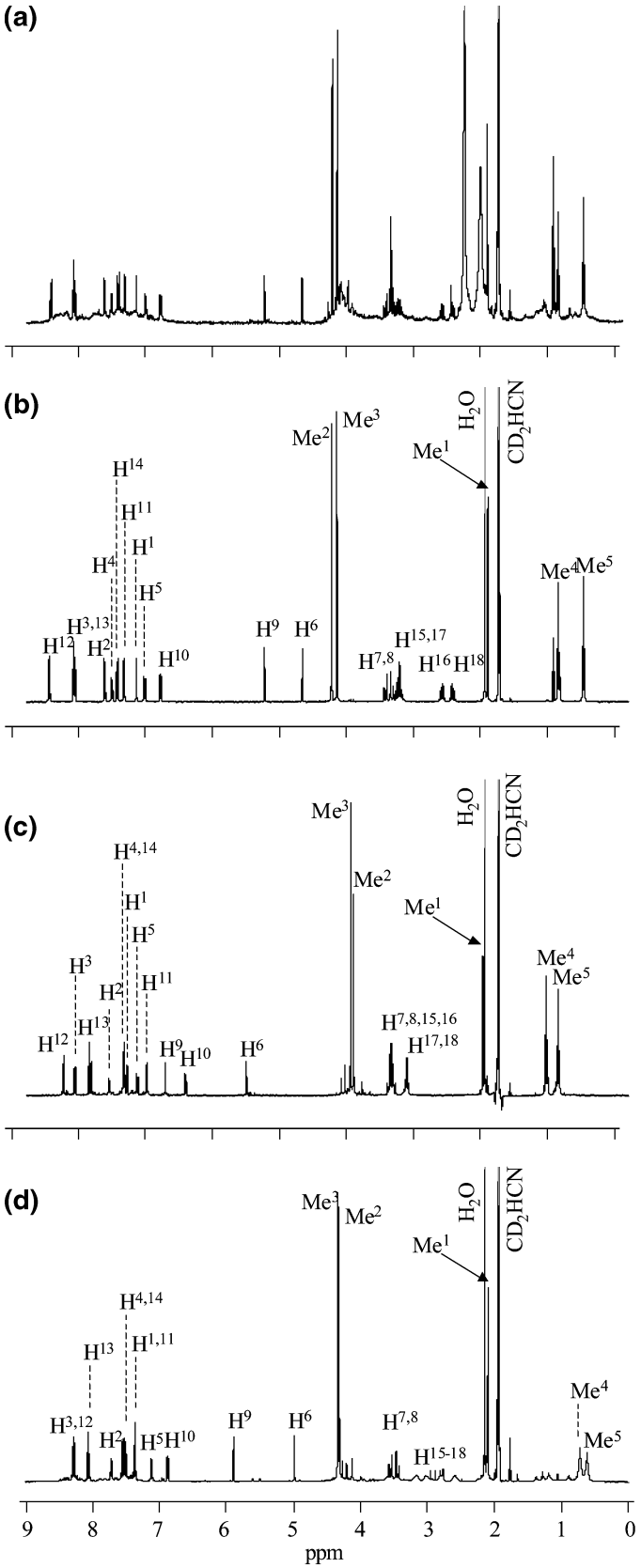

Figure 2. ^{1}H NMR spectra of (a) crude *HHH*-[RuLu(**L5**)$_3$]$^{5+}$ and *HHT*-[Ru(**L5**)$_3$]$^{2+}$, (b) *HHH*-[RuLu(**L5**)$_3$]$^{5+}$ after purification, (c) *HHH*-[Ru(**L5**)$_3$]$^{2+}$, and (d) *HHH*-[RuCa(**L5**)$_3$]$^{4+}$ (CD$_3$CN, 293 K, numbering in Scheme 1).

(10) Piguet, C.; Bernardinelli, G.; Hopfgartner, G. *Chem. Rev.* **1997**, *97*, 2005−2062. (b) Albrecht, M. *Chem. Rev.* **2001**, *101*, 3457−3497.
(11) Torelli, S.; Delahaye, S.; Hauser, A.; Bernardinelli, G.; Piguet, C. *Chem.—Eur. J.* **2004**, *10*, 3503−3516.
(12) (a) Rigault, S.; Piguet, C.; Bernardinelli, G.; Hopfgartner, G. *Angew. Chem., Int. Ed.* **1998**, *37*, 169−172. (b) Rigault, S.; Piguet, C.; Bernardinelli, G.; Hopfgartner, G. *J. Chem. Soc., Dalton Trans.* **2000**, 4587−4600.

Table 1. ^{1}H NMR Chemical Shifts (with Respect to TMS) for Ligand **L5** and Its Complexes *HHH*-[RuLu(**L5**)3]$^{5+}$, *HHH*-[Ru(**L5**)$_3$]$^{2+}$, and *HHH*-[RuCa(**L5**)$_3$]$^{4+}$ in CD_3CN at 293 K (Numbering in Scheme 1)

	bidentate binding site								
	Me^1	Me^2	H^1	H^2	H^3	H^4	H^5	H^6	$H^{7,8}$
L5[a]	2.42	4.23	8.51	7.64	8.26	7.33	7.20	7.71	4.29
[RuLu(**L5**)$_3$]$^{5+}$	2.10	4.43	7.35	7.82	8.28	7.71	7.22	4.87	3.55 3.61
[Ru(**L5**)$_3$]$^{2+}$	2.18	4.11	7.49	7.75	8.27	7.53	7.33	5.71	3.54
[RuCa(**L5**)$_3$]$^{4+}$	2.10	4.33	7.34	7.70	8.25	7.53	7.10	4.98	3.48 3.55

	tridentate binding site										
	Me^3	H^9	H^{10}	H^{11}	H^{12}	H^{13}	H^{14}	$H^{15,16}$	$H^{17,18}$	Me^4	Me^5
L5[a]	4.21	7.69	7.23	7.34	8.38	7.93	7.57	3.61	3.35	1.30	1.13
[RuLu(**L5**)$_3$]$^{5+}$	4.35	5.44	6.99	7.53	8.65	8.28	7.63	3.42, 2.79	3.42, 2.63	1.05	0.67
[Ru(**L5**)$_3$]$^{2+}$	4.13	6.91	6.61	7.20	8.44	8.04	7.53	3.54	3.31	1.23	1.05
[RuCa(**L5**)$_3$]$^{4+}$	4.31	5.89	6.86	7.35	8.28	8.05	7.49	3.17, 2.80	3.00, 2.57	1.05	0.67

[a] Recorded in $CDCl_3$.

preparation of *HHH*-[RuLu(**L5**)$_3$]$^{5+}$ is not negligible. This synthetic process can be followed by ^{1}H NMR spectroscopy for the soluble intermediates and products (Figure 2 and Table 1). Figure 2a shows the crude mixture after the initial assembly step. The upfield shifted signals of the aromatic protons H^6 (4.87 ppm) and H^9 (5.44 ppm) are diagnostic for the formation of the C_3-symmetrical triple-stranded helicate *HHH*-[RuLu(**L5**)$_3$]$^{5+}$ because the wrapping of the three strands puts these protons in the aromatic shielding region of the neighboring ligands in the same complex.[11,13] The remaining large number of small peaks can be assigned to the low-symmetrical isomer *HHT*-[Ru(**L5**)$_3$]$^{2+}$, while the insoluble part which was filtered prior to the NMR spectrum being recorded, is tentatively attributed to polymetallic oligomers summarized by the generic label [Ru$_2$(**L5**)$_2$](CF$_3$SO$_3$)$_4$, in analogy with some closely related observations leading to [Zn$_2$(**L5**)$_2$](CF$_3$SO$_3$)$_4$.[13] The decrease in polarity produced by the addition of $CHCl_3$ to the soluble crude mixture containing *HHH*-[RuLu(**L5**)$_3$]$^{5+}$ and *HHT*-[Ru(**L5**)$_3$]$^{2+}$ induces selective precipitation of the most-charged species, and pure *HHH*-[RuLu(**L5**)$_3$](CF$_3$SO$_3$)$_5$ can be separated by filtration. Its redissolution in acetonitrile confirms the existence of the C_3-symmetrical *HHH*-[RuLu(**L5**)$_3$]$^{5+}$ as the single species in solution (Figure 2b). The standard decomplexation of Lu(III) with EDTA^{4-} provides the monometallic noncovalent tripod *HHH*-[Ru(**L5**)$_3$]$^{2+}$ (Figure 2c),[8,12] in which only H^6 (5.71 ppm) is still affected by the wrapping of the strands about Ru(II), whereas H^9 (6.91 ppm) appears in the standard domain for an aromatic proton in a diamagnetic complex because the tridentate binding units are noncoordinated (see Figure 1b for a structural scheme). Finally, recombination with Ca^{2+} restores the closely packed and rigid C_3-symmetrical triple-stranded organization of the strands in *HHH*-[RuCa(**L5**)$_3$]$^{4+}$, as measured by the low-field resonances of H^6 (4.98 ppm) and H^9 (5.89 ppm) and the diastereotopic methylene protons $H^{7,8}$, $H^{15,16}$, and $H^{17,18}$ (Figure 2d).[11−13]

Elemental analyses confirm the isolation of *HHH*-[Ru(**L5**)$_3$](CF$_3$SO$_3$)$_2$·2.5H$_2$O (1), *HHH*-[RuCa(**L5**)$_3$](CF$_3$SO$_3$)$_4$·7H$_2$O (**2**), and *HHH*-[RuLu(**L5**)$_3$](CF$_3$SO$_3$)$_5$·3.5H$_2$O (**3**) in the solid state, while the previously reported crystal structure of **3** unambigously established the triple helical character of these complexes, in which the metallic sites are separated by ~9.0 Å (d_{RuLu} = 9.08 Å in **3**, see Figure 1a).[11]

Ru-Centered Redox Processes Occurring in [Ru(L5)$_3$](CF$_3$SO$_3$)$_2$, [RuCa(L5)$_3$](CF$_3$SO$_3$)$_4$, and [RuLu(L5)$_3$](CF$_3$SO$_3$)$_5$. The electrochemical Ru(III)/Ru(II) reduction process described in eq 2 and schematically illustrated in Figure 1a has been investigated by cyclic voltammetry (Figure 3 and Table 2). The scan-rate independent 60−80 mV separation between the anodic and cathodic peaks implies the existence of reversible electron-transfer processes, for which the electrochemical potentials $E^0_{Ru(III)A/Ru(II)A}$ can be estimated using standard methods

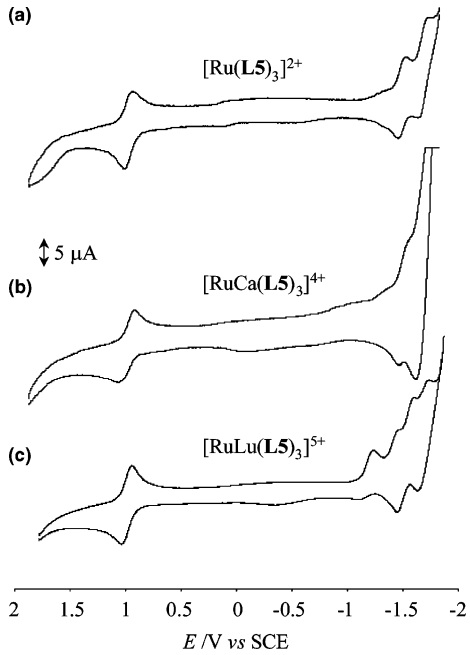

Figure 3. Cyclic voltamograms of (a) [Ru(**L5**)$_3$]$^{2+}$, (b) [RuCa(**L5**)$_3$]$^{4+}$, and (c) [RuLu(**L5**)$_3$]$^{5+}$ (0.5 mM, CH_3CN + 0.1 mM Bu_4NPF_6, 298 K).

(13) Piguet, C.; Bünzli, J.-C. G.; Bernardinelli, G.; Hopfgartner, G.; Petoud, S.; Schaad, O. *J. Am. Chem. Soc.* **1996**, *118*, 6681−6697.

Table 2. Experimental Electrochemical Reduction Potentials ($E^0_{Ru(III)A/Ru(II)A}$), Free Energies of Electron Transfer ($\Delta G^0_{et,sol}$), Hydrodynamic Radii (r_h), and Calculated Free Energies of Solvation ($\Delta_{solv}G^0$) for *HHH*-[Ru(**L5**)$_3$]$^{3+/2+}$, *HHH*-[RuCa(**L5**)$_3$]$^{5+/4+}$, and *HHH*-[RuLu(**L5**)$_3$]$^{6+/5+}$ (Acetonitrile, 298 K)

	$E^0_{Ru(III)A/Ru(II)A}$[a] (V)	$E^a_p - E^c_p$[b] (mV)	$\Delta G^0_{et,sol}$[c] (kJ mol^{-1})	$r_{h,Ru(II)A}$[d] (Å)	$\Delta_{solv}G^0_{Ru(III)A}$[e] (kJ mol^{-1})	$\Delta_{solv}G^0_{Ru(II)A}$[e] (kJ mol^{-1})
[Ru(**L5**)$_3$]$^{3+/2+}$	0.97(1)	60(5)	−94(2)	7.90(5)	−771(4)	−342(3)
[RuCa(**L5**)$_3$]$^{5+/4+}$	0.96(1)	70(7)	−93(2)	8.10(5)	−2091(12)	−1338(7)
[RuLu(**L5**)$_3$]$^{6+/5+}$	0.98(1)	80(5)	−95(2)	8.10(5)	−3012(19)	−2091(12)

[a] Reduction potential vs standard calomel electrode (SCE) in CH_3CN + 0.1 mM $^nBu_4NPF_6$ determined by cyclic voltammetry. [b] Separation between the anodic and cathodic peaks. [c] Calculated with eq 3. [d] Experimental hydrodynamic radius determined by NMR DOSY (CD_3CN, 298 K). [e] Solvation energies calculated with eq 6 for the Ru(III) and Ru(II) forms, respectively.

(Table 2, columns 2 and 3; we assume that the diffusion coefficients of the analogous Ru(III) and Ru(II) forms are identical within each redox pair).[14]

$$[Ru^{III}A(\mathbf{L5})_3]^{(3+z)+} + \bar{e} \rightarrow [Ru^{II}A(\mathbf{L5})_3]^{(2+z)+} \quad E^0_{Ru(III)A/Ru(II)A} \quad (2)$$

Surprisingly, the Ru(III)/Ru(II) potentials measured in the complexes $[Ru^{III}A(\mathbf{L5})_3]^{(3+z)+}$ (A = Ø, z = 0; A = Ca(II), z = 2; A = Lu(III), z = 3) and obviously the associated free energies of electron transfer in solution $\Delta G^0_{et,sol}$ (eq 3, n = 1 is the number of exchanged electrons and F = 96490 C mol^{-1} is the Faraday constant), do not depend on the presence of the spectator cation located at 9.08 Å from the ruthenium center (Table 2, column 4, and Figure 3).[11]

$$\Delta G^0_{et,sol} = -nFE^0_{Ru(III)A/Ru(II)A} \quad (3)$$

Model and Interpretation of the Electrostatic Intermetallic Communication in [Ru(L5)$_3$](CF$_3$SO$_3$)$_2$, [RuCa(L5)$_3$](CF$_3$SO$_3$)$_4$, and [RuLu(L5)$_3$](CF$_3$SO$_3$)$_5$. Taking into account a continuous relative dielectric permittivity ϵ_r = 36.1 in acetonitrile,[15] the integration of Coulomb eq 1 gives eq 4, in which W^{extra}_{elec} is the extra electrostatic work provided by the attachment of an additional electron (z_1 = 1) to Ru(III) in the bimetallic complexes $[Ru^{III}A(\mathbf{L5})_3]^{(3+z)+}$ (i.e., the redox process shown in Figure 1a), because of the additional attractive effect of the spectator cation possessing a z_2 charge located at d = 9.08 Å.

$$W^{extra}_{elec} = -\frac{N_{av}z_1z_2e^2}{4\pi\epsilon_0\epsilon_r d} \quad (4)$$

In absence of a spectator cation, z_2 = 0, and we calculate $W^{extra}_{elec}([Ru^{III}(\mathbf{L5})_3]^{3+})$ = 0. We can similarly predict that $W^{extra}_{elec}([Ru^{III}Ca(\mathbf{L5})_3]^{5+})$ = −8.5 kJ/mol (z_2 = 2) and $W^{extra}_{elec}([Ru^{III}Lu(\mathbf{L5})_3]^{6+})$ = −12.8 kJ/mol (z_2 = 3), which translate, using eq 3, into cathodic shifts of $\Delta E^{cath}_{shift}([Ru^{III}(\mathbf{L5})_3]^{3+})$ = 0 mV, $\Delta E^{cath}_{shift}([Ru^{III}Ca(\mathbf{L5})_3]^{5+})$ = 89 mV, and $\Delta E^{cath}_{shift}([Ru^{III}Lu(\mathbf{L5})_3]^{6+})$ = 133 mV, respectively. Such large shifts for reversible redox processes cannot escape detection by cyclic voltammetry, and we conclude that this unavoidable electrostatic effect is probably masked in our electrochemical experiments by the change in the solvation energies occurring upon reduction. To get rid of the solvent effects and to restore predictable electrostatic trends, the Born−Haber cycle shown in Scheme 2 has been used to estimate the free energy of the reduction process occurring in the gas phase ($\Delta G^0_{et,gas}$).[16] The latter term is related to the same experimentally accessible process occurring in solution ($\Delta G^0_{et,sol}$, Table 2, column 4) via the standard free energies of solvation of the complex cations $[Ru^{III}A(\mathbf{L5})_3]^{(3+z)+}$ ($\Delta_{solv}G^0_{Ru(III)A}$) and $[Ru^{II}A(\mathbf{L5})_3]^{(2+z)+}$ ($\Delta_{solv}G^0_{Ru(II)A}$) according to eq 5.

Scheme 2. Thermodynamic Born−Haber Cycle for the Ru(III)/Ru(II) Reduction Process Occurring in $[RuA(\mathbf{L5})_3]^{(3+z)+}$ (A = Ø, z = 0; A = Ca, z = 2; A = Lu, z = 3)

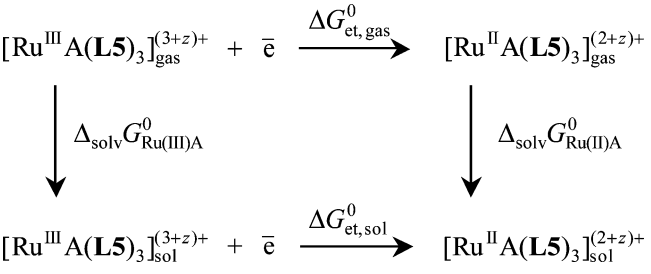

$$\Delta G^0_{et,gas} = \Delta G^0_{et,sol} + \Delta_{solv}G^0_{Ru(III)A} - \Delta_{solv}G^0_{Ru(II)A} \quad (5)$$

To estimate the free energies of solvation required in eq 5, we have used the famous eq 6, proposed by Born in 1920 for a spherical ion in a dielectric continuum.[17] The first term of eq 6 corresponds to the notional process of charging a neutral particule having a radius r of the ion concerned in the gas phase (ϵ_r = 1), while the second term refers to the same process performed in solvent (ϵ_r = 36.1 in acetonitrile). The difference between these two self-energies is interpreted as the Gibbs energy of solvation of the ion in the solvent medium (z is the total charge of the ion in electrostatic units).[18]

$$\Delta_{solv}G^0 = -\frac{N_{av}z^2e^2}{8\pi\epsilon_0 r} + \frac{N_{av}z^2e^2}{8\pi\epsilon_0\epsilon_r r} \quad (6)$$

Except for large-sized monatomic ions, the hypothesis of a spherical ion in the dielectric continuum required in eq 6 is rarely met for real charged systems in chemistry,[18] and a number of modifications and adaptations have been proposed to obtain satisfying semiquantitative solvation energies for

(14) Bard, A. J.; Faulkner, L. R. *Electrochemical Methods*; John Wiley & Sons: New York, 1980; Vol. 6, pp 213−236.
(15) Geary, W. J. *Coord. Chem. Rev.* **1971**, *7*, 81−122.
(16) Chen, H. L.; Ellis, P. E.; Wijesekera, T.; Hagan, T. E.; Groh, S. E.; Lyons, J. E.; Ridge, D. P. *J. Am. Chem. Soc.* **1994**, *116*, 1086−1089.
(17) Born, M. *Z. Phys.* **1920**, *1*, 45−48.
(18) Conway, B. E. In *Modern Aspects of Electrochemistry*; Conway, B. E., White, R. E., Eds.; Kluwer Academic/Plenum Publishers: New York, 2002; pp 295−323.

Chart 2

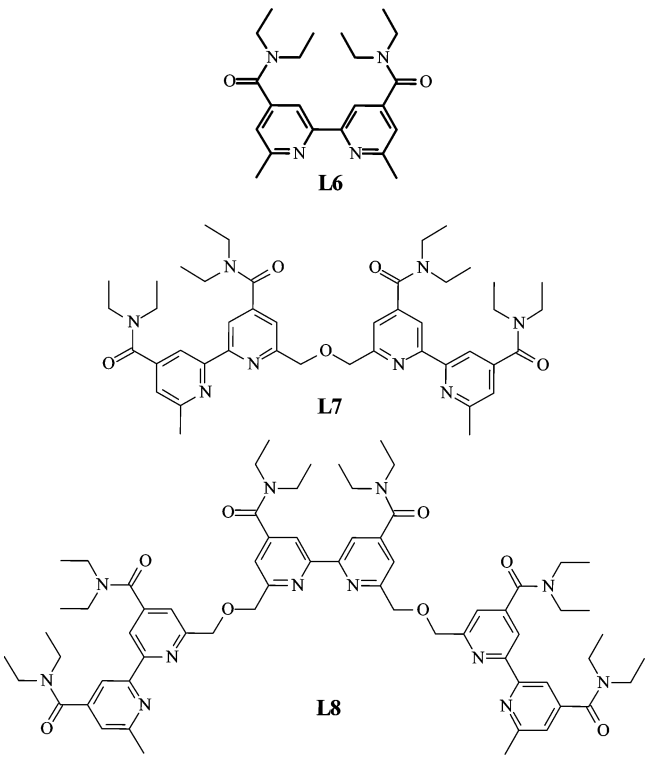

complex ions.[19−21]As far as the solvation of the cations $[Ru^{III}A(\mathbf{L5})_3]^{(3+z)+}$ and $[Ru^{II}A(\mathbf{L5})_3]^{(2+z)+}$ in acetonitrile are concerned, a series of reasonable assumptions can be made for the estimation of their solvation energies. (1) It has been shown by diffusion NMR measurements in polar solutions ($\epsilon_r \geq 25-30$) that the formation of ion pairs can be neglected for singly charged cations larger than 4.5−5.0 Å, which thus diffuse independently in solution.[22] The recent determination of reliable molecular sizes for the series of double-stranded helicates $[Cu(\mathbf{L6})_2]^+$, $[Cu_2(\mathbf{L7})_2]^{2+}$, and $[Cu_3(\mathbf{L8})_2]^{3+}$ in acetonitrile/chloroforme mixtures by diffusion measurements suggests that these multiply charged cations also diffuse independently in solution (Chart 2),[23] an assumption retained for our analogous RuA triple-stranded helicates. (2) The breakdown of the dielectric continuum associated with the polarization of the solvent molecules close to the cation can be neglected when $r > 4.5-5.0$ Å, a situation encountered for the RuA helicates.[19] (3) Small deviations from an ideal sphere for the ions (ellipse or cylinder) has only minor impact on their solvation energies[20] and on their autodiffusion coefficients.[24] For elliptic or cylindrical length/width ratios $p \leq 3$, the approximation of a sphere remains valid;[24] a situation which is encountered for $[Ru^{III}A(\mathbf{L5})_3]^{(3+z)+}$ and $[Ru^{II}A(\mathbf{L5})_3]^{(2+z)+}$ because $p \approx 1.6$ in the crystal structure of $[RuLu(\mathbf{L5})_3]^{5+}$ (Figure S1a, Supporting Information).[11] (4) A simple inspection of eq 6 indicates that, in polar solvents ($\epsilon_r \geq 25-30$), the second term can be neglected, and $\Delta_{solv}G^0$ mainly depends on z^2/r in the gas phase.[18,21] We conclude that eq 6 can be used for an approximate estimation of the solvation energies of the cations $[Ru^{III}A(\mathbf{L5})_3]^{(3+z)+}$ and $[Ru^{II}A(\mathbf{L5})_3]^{(2+z)+}$. However, if the total charges z borne by these cations in the gas phase are obvious, the estimation of their pseudospherical radii is less straightforward. According to Stokes,[19] the ionic radius of a monatomic ion in the gas-phase significantly deviates from its value calculated by using Shannon's definition in the solid state.[25] A better estimation considers the radius of the noble gas possessing the same electronic configuration, to which a quantum scaling factor is applied for taking into account Slater's screening effects.[19] Following this principle, the size of large cations in the gas-phase could be approached by consideration of the volume limited by the Connolly surface constructed around the molecular structure in the crystalline state.[26] For the pseudospherical cation $[Ru(2,2'\text{-bipyridine})_3]^{2+}$,[27] the Connolly surface, built from the crystal structure, limits a total volume $V_{Connolly} = 450.4$ Å^3, corresponding to $r([Ru(bipy)_3]^{2+}) = \sqrt[3]{3V_{Connolly}/4\pi} = 4.75$ Å if we assume a spherical shape for this cation (Figure S1b, Supporting Information). A related calculation is more debatable for the less-spherical cations $[Ru^{III}A(\mathbf{L5})_3]^{(3+z)+}$ and $[Ru^{II}A(\mathbf{L5})_3]^{(2+z)+}$ (Figure S1a, Supporting Information), and we have thus followed Einstein's original suggestion of using a self-diffusion coefficient in solution for the determination of the real size of molecules.[28] For large solute particles ($r/r_{solvent} \geq 0.5$), the Stokes−Einstein relationship (eq 7) holds,[29] and the auto-diffusion coefficient, D, is proportional to r^{-1}, where r is the radius of the moving ion in solution and η is the viscosity of the solvent. Moreover, we assume in our semiquantitative approach that large cations such as $[Ru^{III}A(\mathbf{L5})_3]^{(3+z)+}$ and $[Ru^{II}A(\mathbf{L5})_3]^{(2+z)+}$ diffuse in acetonitrile with sufficiently thin solvation spheres that r measured in solution can be taken as a satisfying approximation for the effective radius of the gas-phase cations. Finally, the removal of one electron from a poorly π-bonding Ru-centered orbital on going from $[Ru^{II}A(\mathbf{L5})_3]^{(2+z)+}$ to $[Ru^{III}A(\mathbf{L5})_3]^{(3+z)+}$ has a negligible effect on the ionic radius, and we can safely claim that $r([Ru^{II}A(\mathbf{L5})_3]^{(2+z)+}) \approx r([Ru^{III}A(\mathbf{L5})_3]^{(3+z)+})$.

$$D = \frac{RT}{6\pi N_{av}\eta r} \tag{7}$$

The experimental determination of diffusion coefficients for $[RuA(\mathbf{L5})_3]^{(2+z)+}$ (A = Ø, $z = 0$; A = Ca(II), $z = 2$; A = Lu(III), $z = 3$) using ^{1}H diffusional ordered spectroscopy

(19) Stokes, R. H. *J. Phys. Chem.* **1964**, *86*, 979−982.
(20) Abe, T. *Bull. Chem. Soc. Jpn.* **1991**, *64*, 3035−3038.
(21) Kumar, A. *J. Phys. Soc. Jpn.* **1992**, *61*, 4247−4250.
(22) Martinez-Viviente, E.; Pregosin, P. S.; Vial, L.; Herse, C.; Lacour, J. *Chem.−Eur. J.* **2004**, *10*, 2912−2918.
(23) Allouche, L.; Marquis, A.; Lehn, J.-M. *Chem.−Eur. J.* **2006**, *12*, 7520−7525.
(24) (a) Broersma, S. *J. Chem. Phys.* **1960**, *32*, 1626−1631. (b) Doi, M.; Edwards, S. F. *The Theory of Polymer Dynamics*; Oxford University Press: Oxford, U.K., 1986; Vol. 73, pp 289−303. (c) Galantini, L.; Pavel, N. V. *J. Chem. Phys.* **2003**, *118*, 2865−2872. (d) Yamakawa, H.; Tanaka, G. *J. Chem. Phys.* **2006**, *57*, 1537−1546.
(25) Shannon, R. D. *Acta Crystallogr.* **1976**, *A32*, 751−767.
(26) (a) Connolly, M. L. *Science* **1983**, *221*, 709−713. (b) Connolly, M. l. *J. Appl. Crystallogr.* **1983**, *16*, 548−553.
(27) Harrowfield, J. M.; Sobolev, A. N. *Aust. J. Chem.* **1994**, *47*, 763−767.
(28) (a) Einstein, A. *Ann. Phys.* **1906**, *19*, 289−306. (b) (a) Einstein, A. *Ann. Phys.* **1906**, *19*, 371−381.
(29) Sharma, M.; Yashonath, S. *J. Phys. Chem. B* **2006**, *110*, 17207−17211.

Table 3. Gibbs Free Energy ($\Delta G^0_{et,gas}$) for the Ru(III)/Ru(II) Reduction Process Occurring in the Gas Phase and Experimental (W^{extra}_{elec}) and Calculated ($W^{extra}_{elec,calcd}$) Extra Electrostatic Work for *HHH*-$[Ru(\mathbf{L5})_3]^{3+/2+}$, *HHH*-$[RuCa(\mathbf{L5})_3]^{5+/4+}$, and *HHH*-$[RuLu(\mathbf{L5})_3]^{6+/5+}$ (Acetonitrile, 298 K)

	$\Delta G^0_{et,gas}$ [a] (kJ mol^{-1})	W^{extra}_{elec} [b] (kJ mol^{-1})	$W^{extra}_{elec,calcd}$ [c] (kJ mol^{-1})
$[Ru(\mathbf{L5})_3]^{3+/2+}$	−523	0	0
$[RuCa(\mathbf{L5})_3]^{5+/4+}$	−846	−323	−306
$[RuLu(\mathbf{L5})_3]^{6+/5+}$	−1016	−493	−459

[a] Calculated with eq 5. [b] Calculated with eq 8. [c] Calculated with eq 4 ($\epsilon_r = 1$, $d = 9.08$ Å).

(DOSY) in CD_3CN at 298 K gives $D([Ru(bipy)_3]^{2+}) = 13.6(4) \times 10^{-10}$ m^2 s^{-1}, $D([Ru(\mathbf{L5})_3]^{2+}) = 8.2(1) \times 10^{-10}$ m^2 s^{-1}, and $D([RuCa(\mathbf{L5})_3]^{4+}) = D([RuLu(\mathbf{L5})_3]^{5+}) = 8.0(1) \times 10^{-10}$ m^2 s^{-1}. The first value can be compared with the value, $D([Cu(\mathbf{L6})_2]^+) = 12.5 \times 10^{-10}$ m^2 s^{-1}, reported for a pseudotetrahedral Cu(I) cation with the bulky ligand **L6**,[23] while the autodiffusion coefficients for the triple-stranded ruthenium helicates are similar to that, $D([Cu_2(\mathbf{L7})_2]^{2+}) = 8.8 \times 10^{-10}$ m^2 s^{-1}, measured for an analogous binuclear double-stranded helicate in the same experimental conditions.[23] With $r([Ru(bipy)_3]^{2+}) = 4.75$ Å as a reference, eq 7 gives $r([Ru(\mathbf{L5})_3]^{2+}) = 7.9$ Å and $r([RuCa(\mathbf{L5})_3]^{4+}) = r([RuLu(\mathbf{L5})_3]^{5+}) = 8.1$ Å (Table 2, column 5), in fair agreement with value, $r([Cu_2(\mathbf{L7})_2]^{2+}) = 7.2$ Å, calculated for the related double-stranded helicate in which the two cations are only separated by 5.6 Å.[23] The introduction of these cationic radii in eq 6 eventually leads to the solvation energies $\Delta_{solv}G^0$ collected in Table 2 (columns 6 and 7).

The introduction of $\Delta_{solv}G^0$ (Table 2, columns 6 and 7) and $\Delta G^0_{et,sol}$ (Table 2, column 4) into eq 5 allows the estimation of the Gibbs energy change accompanying the Ru(III)/Ru(II) reduction process performed in the gas phase ($\Delta G^0_{et,gas}$, Table 3). The latter free energy term, $\Delta G^0_{et,gas}$, can be partitioned between (i) the electrostatic work and the electronic and structural reorganizations accompanying the reduction of the $Ru(III)N_6$ site, $\lambda_{Ru(III)/Ru(II)}$, a contribution which is reasonably assumed to be identical for the three complexes $[Ru(\mathbf{L5})_3]^{3+}$, $[RuCa(\mathbf{L5})_3]^{5+}$ and $[RuLu(\mathbf{L5})_3]^{6+}$, and (ii) the extra electrostatic work, W^{extra}_{elec}, generated by the approach of one electron with respect to the spectator cation located close to the ruthenium center in $[RuCa(\mathbf{L5})_3]^{5+}$ and $[RuLu(\mathbf{L5})_3]^{6+}$ ($d = 9.08$ Å, eq 8).[11]

$$\Delta G_{et,gas}{}^0 = \lambda_{Ru(III)/Ru(II)} + W^{extra}_{elec} \qquad (8)$$

For $[Ru(\mathbf{L5})_3]^{3+}$, $W^{extra}_{elec} = 0$ and thus $\lambda_{Ru(III)/Ru(II)} = \Delta G^0_{et,gas}([Ru(\mathbf{L5})_3]^{3+}) = -523$ kJ mol^{-1}, from which $W^{extra}_{elec}(RuCa) = -323$ kJ mol^{-1} and $W^{extra}_{elec}(RuLu) = -493$ kJ mol^{-1} can be easily calculated with eq 8 and the $\Delta G^0_{et,gas}$ values collected in Table 3. Interestingly, the expected electrostatic trend $|W^{extra}_{elec}(RuCa)| < |W^{extra}_{elec}(RuLu)|$ is qualitatively restored in the gas phase, and these values can be satisfactorially compared with $W^{extra}_{elec,calcd}(RuCa) = -306$ kJ mol^{-1} and $W^{extra}_{elec,calcd}(RuLu) = -459$ kJ mol^{-1} calculated with Coulomb eq 4 in the gas phase ($\epsilon_r = 1$, Table 3). The minor 8% discrepancy between experimental and predicted data in the gas phase is remarkable according to the rough semiquantitative approach used for the estimation of the solvation energies. We thus conclude that the intermetallic communication in $[Ru^{III}A(\mathbf{L5})_3]^{(3+z)+}$ and in $[Ru^{II}A(\mathbf{L5})_3]^{(2+z)+}$ has indeed a simple electrostatic origin in the gas phase, but it is masked in solution by opposite solvation effects which favor the stabilization of highly charged ions.

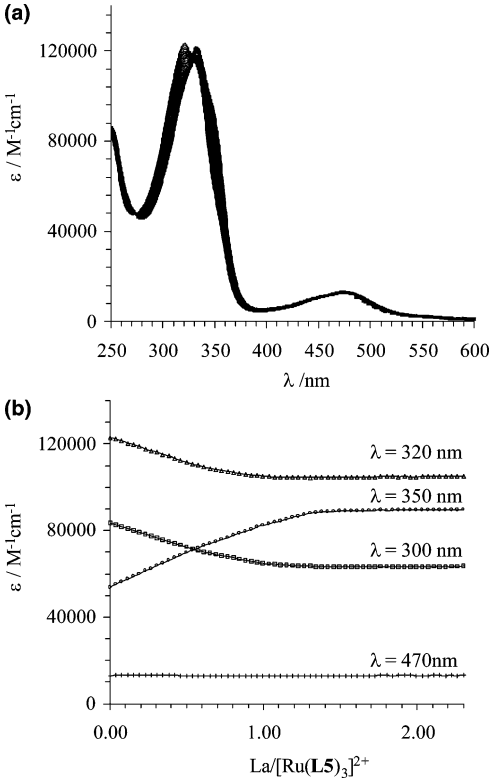

Figure 4. (a) Variation of absorption spectra observed for the spectrophotometric titration of $[Ru(\mathbf{L5})_3]^{2+}$ (10^{-4} mM in acetonitrile) with $La(CF_3SO_3)_3 \cdot 3H_2O$ at 298 K ($La/[Ru(\mathbf{L5})_3]^{2+} = 0.1-2.3$). (b) Corresponding variation of observed molar extinctions at four different wavelengths.

Complexation Processes Occurring in $[RuLn(L5)_3](CF_3SO_3)_5$ and $[CrLn(L5)_3](CF_3SO_3)_6$. Spectrophotometric titrations of $[Ru(\mathbf{L5})_3]^{2+}$ (10^{-4} M, CH_3CN, 298 K) with $Ln(CF_3SO_3)_3 \cdot xH_2O$ (Ln = La, Eu, Gd, Er, Lu; $x = 1-4$) show a smooth evolution of the absorption spectra resulting from the red-shift of the ligand-centered $\pi \rightarrow \pi^*$ transitions occurring upon complexation of the tridentate binding unit to Ln(III), as previously established for the same complexation reaction performed with $[Cr(\mathbf{L5})_3]^{3+}$ instead of $[Ru(\mathbf{L5})_3]^{2+}$ (Figure 4).[8] A single end point is systematically observed for $Ln/[Ru(\mathbf{L5})_3]^{2+} = 1.0$, together with two isosbestic points at 273 and 328 nm, implying the existence of only two species $[Ru(\mathbf{L5})_3]^{2+}$ and $[RuLn(\mathbf{L5})_3]^{5+}$ absorbing in the near UV (Figure 1b). The spectrophotometric data can be satisfyingly fitted with nonlinear least-squares technique to equilibrium 9.[30]

The formation constants, $\log(\beta^{RuLn}_{11}) = 5.2-5.4$, do not vary significantly along the lanthanide series within experi-

(30) (a) Gampp, H.; Maeder, M.; Meyer, C. J.; Zuberbühler, A. *Talanta* **1986**, *33*, 943−951. (b) Gampp, H.; Maeder, M.; Meyer, C. J.; Zuberbühler, A. *Talanta* **1985**, *23*, 1133−1139.

$$[Ru(\mathbf{L5})_3]^{2+} + Ln^{3+} \rightleftharpoons [RuLn(\mathbf{L5})_3]^{5+} \log(\beta_{11}^{RuLn}) \quad (9)$$

mental errors and point to negligible size-discriminating effects (Table 4). Moreover, the $\log(\beta_{11}^{RuLn})$ values are similar to the $\log(\beta_{11}^{CrLn})$ values previously reported for the same complexation processes recorded under the same conditions, but in which the doubly charged tripod $[Ru(\mathbf{L5})_3]^{2+}$ is replaced with the triply charged analogue $[Cr(\mathbf{L5})_3]^{3+}$ (Table 4).[8]

Model and Interpretation of the Electrostatic Intermetallic Communication in $[RuLn(L5)_3](CF_3SO_3)_5$ and $[CrLn(L5)_3](CF_3SO_3)_6$. The experimental formation constants determined for the above-mentioned complexation processes again suggest that the expected increased electrostatic repulsion operating in $[CrLn(\mathbf{L5})_3]^{6+}$ is overcome in solution by the reorganization of the solvent around the cation. This can be modeled by the Born−Haber cycle depicted in Scheme 3, whereby the free energy of complexation in the gas phase ($\Delta G^0_{comp,gas}(MLn)$) is related to that in solution ($\Delta G^0_{comp,sol}(MLn)$) by the balance of the various solvation energies (eqs 10 and 11). Moreover, $\Delta G^0_{comp,gas}(MLn)$ can be partitioned between (i) the sum of the free energies of binding and of reorganization of $[M(\mathbf{L5})_3]^{m+}$ required to accommodate Ln(III), $\delta_{Ln,gas}$, a contribution which is reasonably assumed to be identical for the two noncovalent tridodal receptors $[Ru(\mathbf{L5})_3]^{2+}$ and $[Cr(\mathbf{L5})_3]^{3+}$, and (ii) the extra electrostatic work $W^{extra}_{elec,MLn}$ generated by the approach of the tricationic lanthanide Ln^{3+} from the M^{m+} cations in $[RuLn(\mathbf{L5})_3]^{5+}$ ($m = 2$, $d = 9.08$ Å)[11] and $[CrLn(\mathbf{L5})_3]^{6+}$ ($m = 3$, $d = 9.35$ Å).[31]

$$\Delta G^0_{comp,gas}(RuLn) = \Delta G^0_{comp,sol}(RuLn) + \Delta_{solv}G^0(Ru) + \Delta_{solv}G^0(Ln) - \Delta_{solv}G^0(RuLn) = \delta_{Ln} + W^{extra}_{elec,RuLn} \quad (10)$$

$$\Delta G^0_{comp,gas}(CrLn) = \Delta G^0_{comp,sol}(CrLn) + \Delta_{solv}G^0(Cr) + \Delta_{solv}G^0(Ln) - \Delta_{solv}G^0(CrLn) = \delta_{Ln} + W^{extra}_{elec,CrLn} \quad (11)$$

The difference between eqs 11 and 10 leads to eq 12, in which the variation of the free energy of complexation in the gas phase ($\Delta G^0_{comp,gas}(CrLn) - \Delta G^0_{comp,gas}(RuLn)$) indeed corresponds to the difference of the electrostatic works required for bringing Ln^{3+} close to Cr^{3+} and to Ru^{2+}, respectively, in $[MLn(\mathbf{L5})_3]^{(m+3)+}$ ($W^{extra}_{elec,CrLn} - W^{extra}_{elec,RuLn}$).

$$\Delta G^0_{comp,gas}(CrLn) - \Delta G^0_{comp,gas}(RuLn) = W^{extra}_{elec,CrLn} - W^{extra}_{elec,RuLn} = \Delta G^0_{comp,sol}(CrLn) - \Delta G^0_{comp,sol}(RuLn) + \Delta_{solv}G^0(Cr) - \Delta_{solv}G^0(Ru) + \Delta_{solv}G^0(RuLn) - \Delta_{solv}G^0(CrLn) \quad (12)$$

The introduction of the solvation energies collected in Table 2 (we assume $\Delta_{solv}G^0([Cr(\mathbf{L5})_3]^{3+}) = \Delta_{solv}G^0([Ru(\mathbf{L5})_3]^{3+}) = -771$ kJ mol^{-1} and $\Delta_{solv}G^0([CrLu(\mathbf{L5})_3]^{6+}) = \Delta_{solv}G^0([RuLu(\mathbf{L5})_3]^{6+}) = -3012$ kJ mol^{-1}), together with the free energy of complexation for Ln = Lu ($\Delta G^0_{comp,sol}(MLu) = -30$ kJ mol^{-1}, Table 4) into eq 12 gives $W^{extra}_{elec,CrLu} - W^{extra}_{elec,RuLu} = 492$ kJ mol^{-1}. This experimental value can be fairly compared with the difference of the electrostatic works, each being calculated with Coulomb eq 4 ($z_1 = z_2 = 3$ for $[CrLu(\mathbf{L5})_3]^{6+}$; $z_1 = 2$ and $z_2 = 3$ for $[RuLu(\mathbf{L5})_3]^{5+}$), and eventually combined in eq 13 to give $W^{extra}_{elec,CrLu,calcd} - W^{extra}_{elec,RuLu,calcd} = 419$ kJ mol^{-1} ($d_{RuLu} = 9.08$ Å[11] and $d_{CrLu} = 9.35$ Å).[31]

$$W^{extra}_{elec,CrLn,calcd} - W^{extra}_{elec,RuLn,calcd} = -\frac{3e^2N_{av}}{4\pi\epsilon_0}\left[\frac{2}{d_{RuLn}} - \frac{3}{d_{CrLn}}\right] \quad (13)$$

The slightly larger discrepancy (15%) between the Coulomb prediction in the gas phase (419 kJ mol^{-1}) and the experimental data extracted from the complexation processes described in eq 9 (492 kJ mol^{-1}), compared with the only 8% discrepancy obtained when modeling the reduction process described in eq 5 may have two origins. (1) Four approximate solvation energies (semiquantitative approach) are required to transform $\Delta G^0_{comp,sol}(CrLn) - \Delta G^0_{comp,sol}(RuLn)$ into $\Delta G^0_{comp,gas}(CrLn) - \Delta G^0_{comp,gas}(RuLn)$ (eq 12), while only two are necessary for correlating $\Delta G^0_{et,sol}$ and $\Delta G^0_{et,gas}$ (eq 5). (2) Some polarization of the coordination bonds involving the d-block ions Ru(II) and, especially, Cr(III) may reduce their effective charge in the bimetallic complexes $[MLn(\mathbf{L5})_3]^{(m+z)+}$ and thus affects the predictions obtained with eq 13. This limitation is removed when the extra electrostatic work associated with the reduction process occurring in $[RuLn(\mathbf{L5})_3]^{(3+z)+}$ is considered because the hard 4s- or 4f-block spectator cations are poorly polarizable.

Table 4. Formation Constants $\log(\beta_{11}^{MLn})$ for the Complexes $[MLn(\mathbf{L5})_3]^{(m+3)+}$ According to Equilibrium 9 (M = Ru, $m = 2$; M = Cr, $m = 3$; Ln = La, Nd, Eu, Gd, Er, Lu; Acetonitrile, 298 K)

Ln(III)	$\log(\beta_{11}^{RuLn})$	$\Delta G^0_{comp,sol}(RuLn)$ (kJ mol^{-1})	$\log(\beta_{11}^{CrLn})^a$	$\Delta G^0_{comp,sol}(CrLn)^a$ (kJ mol^{-1})
La	5.4(2)	−31(1)	5.9(3)	−34(2)
Nd			5.4(3)	−31(2)
Eu	5.2(2)	−30(1)		
Gd	5.4(2)	−31(1)	5.4(3)	−31(2)
Er	5.4(2)	−31(1)	5.3(3)	−30(2)
Lu	5.2(2)	−30(1)	5.3(3)	−30(2)

[a] Formation constants taken from ref 8.

Scheme 3. Thermodynamic Born−Haber Cycle for the Complexation of Ln(III) to $[M(\mathbf{L5})_3]^{m+}$ to Give $[MLn(\mathbf{L5})_3]^{(m+3)+}$ (M = Ru, $m = 2$; M = Cr, $m = 3$; Ln = La−Lu)

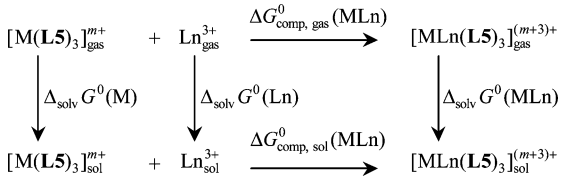

(31) Cantuel, M.; Bernardinelli, G.; Imbert, D.; Bünzli, J.-C. G.; Hopfgartner, G.; Piguet, C. *J. Chem. Soc., Dalton Trans.* **2002**, 1929−1940.

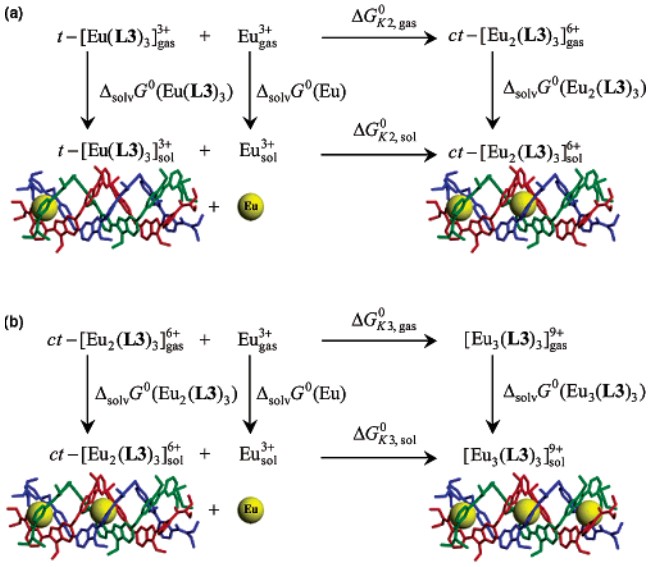

Figure 5. Thermodynamic Born−Haber cycles for the successive complexation of Eu(III) to (a) *t*-[Eu(**L3**)$_3$]$^{3+}$ to give *ct*-[Eu$_2$(**L3**)$_3$]$^{6+}$ and (b) *ct*-[Eu$_2$(**L3**)$_3$]$^{6+}$ to give [Eu$_3$(**L3**)$_3$]$^{9+}$.

Application of the Solvation Model for Unravelling Electrostatic Intermetallic Communication in Solution. The incomprehensible small value $\Delta E^{EuEu}_{exp,sol} = 14$ kJ mol^{-1} characterizing the intermetallic Eu(III)···Eu(III) interaction occurring at 9 Å in the self-assembly of the trinuclear triple-stranded polymetallic helicate [Eu$_3$(**L3**)$_3$]$^{9+}$ in acetonitrile,[5b] which significantly contributes to its surprising stability, can be now re-examined in light of the combination of electrostatic and solvation effects previously developed for the rationalization of redox and complexation processes occurring for d−f bimetallic helicates in solution. Let us consider the formation of the three microspecies *t*-[Eu(**L3**)$_3$]$^{3+}$, *ct*-[Eu$_2$(**L3**)$_3$]$^{6+}$, and [Eu$_3$(**L3**)$_3$]$^{9+}$ characterized by equilibria 14−16 (*c* = central and *t* = terminal correspond to the location of the europium atoms in the central N_9 and terminal N_6O_3 binding sites, respectively, provided by the virtually preorganized receptor (**L3**)$_3$, see Figure 5 for the schematic structures of the complexes).[5b]

$$3\mathbf{L3} + Eu^{3+} \rightleftharpoons t\text{-}[Eu(\mathbf{L3})_3]^{3+} \quad \log(\beta^{t}_{13}) = 16.2 \qquad (14)$$

$$3\mathbf{L3} + 2Eu^{3+} \rightleftharpoons ct\text{-}[Eu_2(\mathbf{L3})_3]^{6+} \quad \log(\beta^{ct}_{23}) = 26.1 \qquad (15)$$

$$3\mathbf{L3} + 3Eu^{3+} \rightleftharpoons [Eu_3(\mathbf{L3})_3]^{9+} \quad \log(\beta^{tct}_{33}) = 34.8 \qquad (16)$$

The associated successive constants K_2 and K_3, corresponding to equilibria 17 and 18, allow the calculation of the free energies for the successive complexation of Eu(III) to *t*-[Eu(**L3**)$_3$]$^{3+}$ ($\Delta G_{K2,sol} = -56.5$ kJ mol^{-1}) and to *ct*-[Eu$_2$(**L3**)$_3$]$^{6+}$ ($\Delta G_{K3,sol} = -49.6$ kJ mol^{-1}) in solution (Figure 5).[5b]

$$t\text{-}[Eu(\mathbf{L3})_3]^{3+} + Eu^{3+} \rightleftharpoons ct\text{-}[Eu_2(\mathbf{L3})_3]^{6+}$$
$$\log(K_2) = \log(\beta^{ct}_{23}) - \log(\beta^{t}_{13}) = 9.9 \qquad (17)$$

$$ct\text{-}[Eu_2(\mathbf{L3})_3]^{6+} + Eu^{3+} \rightleftharpoons [Eu_3(\mathbf{L3})_3]^{9+}$$
$$\log(K_3) = \log(\beta^{tct}_{33}) - \log(\beta^{ct}_{23}) = 8.7 \qquad (18)$$

The solvation energies of each microspecies *t*-[Eu(**L3**)$_3$]$^{3+}$, *ct*-[Eu$_2$(**L3**)$_3$]$^{6+}$, and [Eu$_3$(**L3**)$_3$]$^{9+}$ can be estimated using Born eq 6, thus leading to eqs 19−21, where $\epsilon_r = 36.1$ for acetonitrile and $r = r(t\text{-}[Eu(\mathbf{L3})_3]^{3+}) = 1.25r([Ru(\mathbf{L5})_3]^{2+}) = 10$ Å because the trinuclear triple-stranded helicate [Eu$_3$(**L3**)$_3$]$^{9+}$ possesses three equally spaced metals, while the bimetallic analogue [RuLn(**L5**)$_3$]$^{5+}$ displays only two metals separated by the same distance. The 1.25 ratio corresponds to the average value established by NMR diffusion measurements recorded on going from the binuclear double-stranded helicate [Cu$_2$(**L7**)$_2$]$^{2+}$ to the trinuclear analogue [Cu$_3$(**L8**)$_2$]$^{3+}$ (Chart 2) and for closely related systems.[23] Finally, the stepwise rigidification of the triple helix associated with the successive reaction of Eu(III) with *t*-[Eu(**L3**)$_3$]$^{3+}$ to give *ct*-[Eu$_2$(**L3**)$_3$]$^{6+}$ and finally [Eu$_3$(**L3**)$_3$]$^{9+}$ (Figure 5) produces a stepwise increase of ∼10% in the ionic radii (eqs 19−21) as observed when Ln(III) cooordinates to [Ru(**L5**)$_3$]$^{2+}$ to give [RuLn(**L5**)$_3$]$^{5+}$.

$$\Delta_{solv}G^0(Eu(\mathbf{L3})_3) = -\frac{9N_{av}e^2}{8\pi\epsilon_0 r}\left(1-\frac{1}{\epsilon_r}\right) = -607 \text{ kJ mol}^{-1} \qquad (19)$$

$$\Delta_{solv}G^0(Eu_2(\mathbf{L3})_3) = -\frac{36N_{av}e^2}{8\pi\epsilon_0 (1.1r)}\left(1-\frac{1}{\epsilon_r}\right) = -2208 \text{ kJ mol}^{-1} \qquad (20)$$

$$\Delta_{solv}G^0(Eu_3(\mathbf{L3})_3) = -\frac{81N_{av}e^2}{8\pi\epsilon_0 (1.2r)}\left(1-\frac{1}{\epsilon_r}\right) = -4554 \text{ kJ mol}^{-1} \qquad (21)$$

According to the thermodynamic Born−Haber cycles depicted in Figure 5, the Gibbs free energy for the successive complexation of Eu(III) to *t*-[Eu(**L3**)$_3$]$^{3+}$ (equilibria 17 and 18) in the gas phase can be estimated with eqs 22 and 23. Since the affinity of Eu(III) for the N_9 and N_6O_3 coordination sites is known to be very similar,[32,33]The gas-phase free energies of successive complexation can be partitioned between (i) the intermolecular free energy of connection of the entering Eu(III) in the nine-coordinate site δ_{comp}, a contribution which is reasonably assumed to be identical for the two successive coordination processes, (ii) the extra electrostatic work $W^{extra}_{elec,adjacent}$ for the approach of two adjacent Eu^{3+} in *ct*-[Eu$_2$(**L3**)$_3$]$^{6+}$ and in [Eu$_3$(**L3**)$_3$]$^{6+}$ ($d = 9$ Å)[32] and (iii) the extra electrostatic work $W^{extra}_{elec,distal}$ for the approach of two distal Eu^{3+} in [Eu$_3$(**L3**)$_3$]$^{6+}$ ($d = 18$ Å, eqs 22 and 23).[32]

The difference in free energy of these two successive complexation processes is given in eq 24.

(32) (a) Floquet, S.; Ouali, N.; Bocquet, B.; Bernardinelli, G.; Imbert, D.; Bünzli, J.-C. G.; Hopfgartner, G.; Piguet, C. *Chem.—Eur. J.* **2003**, *9*, 1860−1875. (b) Floquet, S.; Borkovec, M.; Bernardinelli, G.; Pinto, A.; Leuthold, L.-A.; Hopfgartner, G.; Imbert, D.; Bünzli, J.-C. G.; Piguet, C. *Chem.—Eur. J.* **2004**, *10*, 1091−1105.
(33) (a) Piguet, C.; Borkovec, M.; Hamacek, J.; Zeckert, K. *Coord. Chem. Rev.* **2005**, *249*, 705−726. (b) Hamacek, J.; Borkovec, M.; Piguet, C. *Dalton Trans.* **2006**, 1473−1490.

$$\Delta G^0_{K2,gas} = \Delta G^0_{K2,sol} + \Delta_{solv}G^0(Eu(\mathbf{L3})_3) + \Delta_{solv}G^0(Eu) - \Delta_{solv}G^0(Eu_2(\mathbf{L3})_3) = \delta_{comp} + W^{extra}_{elec,adjacent} \quad (22)$$

$$\Delta G^0_{K3,gas} = \Delta G^0_{K3,sol} + \Delta_{solv}G^0(Eu_2(\mathbf{L3})_3) + \Delta_{solv}G^0(Eu) - \Delta_{solv}G^0(Eu_3(\mathbf{L3})_3) = \delta_{comp} + W^{extra}_{elec,adjacent} + W^{extra}_{elec,distal} \quad (23)$$

$$\Delta G^0_{K3,gas} - \Delta G^0_{K2,gas} = \Delta G^0_{K3,sol} - \Delta G^0_{K2,sol} + 2\Delta_{solv}G^0(Eu_2(\mathbf{L3})_3) - \Delta_{solv}G^0(Eu(\mathbf{L3})_3) - \Delta_{solv}G^0(Eu_3(\mathbf{L3})_3) = W^{extra}_{elec,distal} \quad (24)$$

The introduction of eqs 19−21, together with the experimental values $\Delta G_{K2,sol} = -56.5$ kJ mol^{-1} and $\Delta G_{K3,sol} = -49.6$ kJ mol^{-1}, into eq 24 leads to $\Delta G^0_{K3,gas} - \Delta G^0_{K2,gas} = 752$ kJ mol^{-1}, a value which can be compared with the $W^{extra}_{elec,distal} = 694$ kJ mol^{-1} value calculated with the simple Coulomb eq 4 in the gas phase ($z_1 = z_2 = 3$, $\epsilon_r = 1$, $d = 18$ Å).[32] Again, the straightforward electrostatic model is satisfying within 10% for the rationalization of intermetallic interactions in molecules, according that semiquantitative solvation energies are explicitely considered. Finally, it is interesting to estimate the standard intermetallic parameter $\Delta E^{EuEu}_{exp,gas}$, reflecting the adjacent interactions between two Eu(III) cations in the gas-phase complex, to compare it with its apparent small values found in solution $\Delta E^{EuEu}_{exp,sol} = 14$ kJ mol^{-1}. Application of the site binding model[32,33] to equilibria 14−16 in the gas phase gives eqs 25−27,[33] from which the successive constants K_2 (eq 28) and K_3 (eq 29), corresponding to equilibria 17 and 18 in the gas phase, can be calculated (k is the specific affinity of Eu(III) for a nine-coordinate binding site and $u^{EuEu} = e^{-\Delta E^{EuEu}_{exp,gas}/RT}$ is the Boltzmann factor containing the intermetallic interaction parameter $\Delta E^{EuEu}_{exp,gas}$).

$$\beta^t_{13} = 2k \quad (25)$$

$$\beta^{ct}_{23} = 2k^2u^{EuEu} \quad (26)$$

$$\beta^{tct}_{33} = k^3(u^{EuEu})^{5/2} \quad (27)$$

$$K_2 = \beta^{ct}_{23}/\beta^{ct}_{13} = ku^{EuEu} \quad (28)$$

$$K_3 = \beta^{tct}_{33}/\beta^{ct}_{23} = (k/2)(u^{EuEu})^{3/2} \quad (29)$$

The ultimate transformation of the successive stability constants into Gibbs free energy in eq 30 allows the calculation of $\Delta E^{EuEu}_{exp,gas} = 1500$ kJ mol^{-1}, a value in line with the predicted electrostatic interaction $W^{EuEu}_{elec,calcd} = 1388$ kJ mol^{-1}, operating between two triply charged Eu(III) cations separated by 9 Å in the gas phase (eq 4), but completely different from the apparent parameter of $\Delta E^{EuEu}_{exp,sol} = 14$ kJ mol^{-1} found in solution.

$$\Delta G^0_{K3,gas} - \Delta G^0_{K2,gas} = -RT\ln(K_3/K_2) = -\frac{RT}{2}\ln\left(\frac{u^{EuEu}}{2}\right) = RT\ln(2) + \frac{\Delta E^{EuEu}_{exp,gas}}{2} = 752 \text{ kJ mol}^{-1} \quad (30)$$

Experimental Section

Solvents and Starting Materials. These were purchased from Fluka AG (Buchs, Switzerland) and Aldrich and were used without further purification unless otherwise stated. The ligand **L5** was prepared according to a literature procedure.[13] (^{n}Bu$_4$N)$_4$EDTA·6.4H$_2$O was prepared by metathesis of ^{n}Bu$_4$NOH and H$_4$EDTA in water. The trifluoromethanesulfonate salts Ln(CF$_3$SO$_3$)$_3$·xH$_2$O (Ln = La−Lu; $x = 1-4$) were prepared from the corresponding oxides (Rhodia, 99.99%).[34] The Ln content of the solid salts was determined by complexometric titrations with Titriplex III (Merck) in the presence of urotropine and xylene orange.[35] Acetonitrile and dichloromethane were distilled over calcium hydride and ^{n}Bu$_4$NPF$_6$ was recrystallized from hot ethanol.

Preparation of RuCl$_2$(DMSO)$_4$. RuCl$_3$ (600 mg, 2.9 mmol) was dissolved in DMSO (5 mL) and water (160 μL). The mixture was stirred and refluxed for 5 min, and then it was concentrated to half of its original volume. Acetone (50 mL) was added, and the resulting pale yellow solid was filtered, washed with diethyl ether, and dried overnight. The solid was recrystallized from DMSO (2 mL), filtered, washed with diethyl ether, and dried under vacuum to yield RuCl$_2$(DMSO)$_4$ (700 mg, 50%) as pale green-yellow crystals. Calcd for C$_8$H$_{24}$Cl$_2$O$_4$RuS$_4$ (484.5 g mol^{-1}): C, 19.83; H, 4.99. Found: C, 19.76; H, 4.96.

Preparation of Ru(DMSO)$_6$(CF$_3$SO$_3$)$_2$·H$_2$O. RuCl$_2$(DMSO)$_4$ (720 mg, 1.49 mmol) and Ag(CF$_3$SO$_3$) (840 mg, 3.27 mmol, 2.2 equiv) were suspended in toluene (30 mL) and DMSO (420 μL, 5.94 mmol, 4 equiv). The light-protected mixture was refluxed for 1 h. The precipitate containing both AgCl and the insoluble Ru(II) salt was filtered, washed with toluene, and then extracted with methanol at 50 °C for 24 h. The resulting yellow solution was filtered, and the clear filtrate was evaporated to dryness to afford a pale yellow oil. The oil was dissolved in a mixture of acetone and diethyl ether and stored at room temperature. After 24 h, pale yellow crystals of Ru(DMSO)$_6$(CF$_3$SO$_3$)$_2$·H$_2$O (644 mg, 49%) were separated by filtration and dried under vacuum. Calcd for C$_{14}$H$_{36}$F$_6$O$_{12}$RuS$_8$·H$_2$O (886.0 g mol^{-1}): C, 18.97; H, 4.32. Found: C, 18.88; H, 4.30.

Preparation of *HHH*-[RuLu(L5)$_3$](CF$_3$SO$_3$)$_5$·3.5H$_2$O (3). L5 (300 mg, 0.552 mmol, 3 equiv) and Lu(CF$_3$SO$_3$)$_3$·4.6H$_2$O (130 mg, 0.184 mmol, 1 equiv) were suspended in ethanol (24 mL). The mixture was stirred at 50 °C for 30 min until complete dissolution of the solid. Ru(DMSO)$_6$(CF$_3$SO$_3$)$_2$·H$_2$O (163 mg, 0.184 mmol, 1 equiv) was added, and the mixture was stirred and refluxed for 24 h. The red mixture was stored at room temperature without stirring for 24 h. The red precipitate was separated by filtration and washed with ethanol. The resulting solution was evaporated to dryness to give a red solid. Recrystallization from CHCl$_3$/ethanol afforded *HHH*-[RuLu(**L5**)$_3$](CF$_3$SO$_3$)$_5$·3.5H$_2$O (122 mg, 24%) as a red solid. Calcd for C$_{104}$H$_{99}$N$_{21}$F$_{15}$LuO$_{18}$RuS$_5$·3.5H$_2$O (2715.4 g mol^{-1}): C, 46.00; H, 3.93, N, 10.83. Found: C, 45.94; H, 3.56; N, 10.65. ESI-MS: m/z 514.4 ([RuLu(**L5**)$_3$(CF$_3$SO$_3$)]$^{4+}$). ^{1}H NMR (CD$_3$CN): δ 0.67 (t, ^3J = 7.1 Hz, 9H, Me^5), 1.05 (t, ^3J = 7.1 Hz, 9H, Me^4), 2.10 (s, 9H, Me^1), 2.63 (m, 3H, H^{18}), 2.79 (m, 3H, H^{16}), 3.42 (m, 6H, H^{17,18}), 3.61 (dd, ^2J = 16.4 Hz, 6H, H^{7,8}), 4.35 (s, 9H, Me^3), 4.43 (s, 9H, Me^2), 4.87 (s, 3H, H^6), 5.44 (s, 3H, H^9), 6.99 (dd, ^3J = 8.4 Hz, ^4J = 1.4 Hz, 3H, H^{10}), 7.22 (dd, ^3J = 8.5 Hz, ^4J = 1.3 Hz, 3H, H^5), 7.35 (d, ^4J = 1.5 Hz, 3H, H^1), 7.53 (d, ^3J = 8.4 Hz,

(34) Desreux, J.-F. In *Lanthanide Probes in Life, Chemical and Earth Sciences*; Bünzli, J.-C. G., Choppin, G. R., Eds.; Elsevier Publishing Co: Amsterdam, 1989; Chapter 2, p 43.
(35) Schwarzenbach, G. *Complexometric Titrations*; Chapman & Hall: London, 1957; p 8.

3H, H^{11}), 7.63 (d, $^3J = 8.5$ Hz, 3H, H^{14}), 7.71 (dd, $^3J = 8.4$ Hz, $^4J = 1.3$ Hz, 3H, H^4), 7.82 (d, $^3J = 8.0$ Hz, 3H, H^2), 8.28 (m, 6H, $H^{3,13}$), 8.65 ppm (d, $^3J = 8.1$ Hz, 3H, H^3).

Preparation of *HHH*-[Ru(L5)$_3$](CF$_3$SO$_3$)$_2$·2.5H$_2$O (1). A solution of 45 μmol of (^{n}Bu$_4$N)$_4$EDTA·6.4H$_2$O in acetonitrile (1.2 mL) was added dropwise to a solution of *HHH*-[RuLu(**L5**)$_3$]CF$_3$SO$_3$)$_5$·3.5H$_2$O (122 mg, 45 μmol) in acetonitrile (7.5 mL). The mixture was evaporated to dryness. The resulting red solid was dissolved in chloroform, and the pale red precipitate of (^{n}Bu$_4$N)[LuEDTA] was removed by centrifugation. The remaining clear red solution was filtered and concentrated. Precipitation was induced by diffusion of diethyl ether. The precipitate was filtered off and washed with diethyl ether. This procedure was repeated three times to quantitatively remove the excess of ^{n}Bu$_4$N(CF$_3$SO$_3$). The final solid was dissolved in dichloromethane/tetrahydrofuran and then precipitated by the addition of diisopropyl ether. Filtration, followed by washing with diethyl ether and drying under vacuum at 60 °C, yields *HHH*-[RuL$_3$](CF$_3$SO$_3$)$_2$·2.5H$_2$O (76 mg, 81%) as an orange powder. Calcd for C$_{101}$H$_{99}$N$_{21}$F$_6$S$_2$O$_9$Ru·2.5H$_2$O (2075.24 g mol^{-1}): C, 58.46; H, 5.05; N, 14.17. Found: C, 58.47; H, 5.04; N, 14.13. ESI-MS: *m*/*z* 866.8 ([Ru(**L5**)$_3$]$^{2+}$). ^{1}H NMR (CD$_3$CN): δ 1.05 (t, $^3J = 7.1$ Hz, 9H, Me^5), 1.23 (t, $^3J = 7.1$ Hz, 9H, Me^4), 2.18 (s, 9H, Me^1), 3.31 (m, 6H, $H^{17,18}$), 3.54 (m, 12H, $H^{7,8,15,16}$), 4.11 (s, 9H, Me^2), 4.13 (s, 9H, Me^3), 5.71 (s, 3H, H^6), 6.61 (dd, $^3J = 8.4$ Hz, $^4J = 1.5$ Hz, 3H, H^{10}), 6.91 (s, 3H, H^9), 7.20 (d, $^3J = 8.4$ Hz, 3H, H^{11}), 7.33 (dd, $^3J = 8.6$ Hz, $^4J = 1.5$ Hz, 3H, H^5), 7.49 (s, 3H, H^1), 7.53 (m, 6H, $H^{4,14}$), 7.75 (dd, $^3J = 8.4$ Hz, $^4J = 1.3$ Hz, 3H, H^2), 8.04 (t, $^3J = 8.0$ Hz, 3H, H^{13}), 8.27 (d, $^3J = 8.4$ Hz, 3H, H^3), 8.44 (dd, $^3J = 8.0$ Hz, $^4J = 1.0$ Hz, 3H, H^{12}).

Preparation of *HHH*-[RuCa(L5)$_3$](CF$_3$SO$_3$)$_4$·7H$_2$O (2). *HHH*-[Ru(**L5**)$_3$](CF$_3$SO$_3$)$_2$·2.5H$_2$O (15 mg, 7.2 μmol) and Ca(CF$_3$SO$_3$)$_2$ (2.44 mg, 7.2 μmol) were dissolved in dry acetonitrile (7 mL). The mixture was stirred at room temperature for 20 min and then evaporated to dryness. The resulting solid was dissolved in acetonitrile (2 mL), and diisopropylether (7 mL) was added to the solution. The orange powder was filtered, washed with diethyl ether, and dried under vacuum to yield *HHH*-[RuCa(**L5**)$_3$](CF$_3$SO$_3$)$_4$·7H$_2$O (13.3 mg, 74%) as an orange powder. Calcd for C$_{103}$H$_{99}$N$_{21}$F$_{12}$S$_4$O$_{15}$RuCa·7H$_2$O (2494.5 g mol^{-1}): C, 49.59; H, 4.56; N, 11.79. Found: C, 49.54; H, 4.41; N, 11.66. ESI-MS: *m*/*z* 443.3 ([RuCa(**L5**)$_3$]$^{4+}$), 640.6 ([(RuCa(**L5**)$_3$)(CF$_3$SO$_3$)]$^{3+}$), 1035.4 ([(RuCa(**L5**)$_3$)(CF$_3$SO$_3$)$_2$]$^{2+}$), 2219.3 ([(RuCa(**L5**)$_3$)(CF$_3$SO$_3$)$_3$]$^{+}$). ^{1}H NMR (CD$_3$CN): δ 0.62 (t, $^3J = 5.7$ Hz, 9H, Me^5), 0.72 (t, $^3J = 5.8$ Hz, 9H, Me^4), 2.10 (s, 9H, Me^1), 2.54−2.61 (m, 3H, H^{16}), 2.77−2.83 (m, 3H, H^{15}), 2.97−3.03 (m, 3H, H^{17}), 3.14−3.20 (m, 3H, H^{18}), 3.50 (dd, $^2J = 16.3$ Hz, 6H, $H^{7,8}$), 4.31 (s, 9H, Me^3), 4.33 (s, 9H, Me^2), 4.98 (s, 3H, H^6), 5.89 (s, 3H, H^9), 6.86 (dd, $^3J = 8.5$ Hz, $^4J = 1.5$ Hz, 3H, H^{10}), 7.10 (dd, $^3J = 8.4$ Hz, $^4J = 1.3$ Hz, 3H, H^5), 7.34 (s, 3H, H^1), 7.36 (d, $^3J = 8.5$ Hz, 3H, H^{11}), 7.49 (d, $^3J = 7.5$ Hz, 3H, H^{14}), 7.53 (d, $^3J = 8.4$ Hz, 3H, H^4), 7.70 (dd, $^3J = 8.5$ Hz, $^4J = 1.1$ Hz, 3H, H^2), 8.04 (t, $^3J = 8.0$ Hz, 3H, H^{13}), 8.25 (d, $^3J = 8.5$ Hz, 3H, H^3), 8.27 (d, $^3J = 8.2$ Hz, 3H, H^{12}).

Spectroscopic and Analytical Measurements. Electronic spectra in the UV−vis region were recorded at 20 °C from solutions in CH$_3$CN with a Perkin-Elmer Lamβda 900 spectrometer using quartz cells of 0.1 and 1 mm path lengths. Spectrophotometric titrations were performed with a J & M diode array spectrometer (Tidas series) connected to an external computer. In a typical experiment, 20 mL of [Ru(**L5**)$_3$]$^{2+}$ in CH$_3$CN (10^{-4} mol·dm^{-3}) was titrated at 25 °C with a solution of Ln(CF$_3$CO$_2$)$_3$·xH$_2$O (10^{-3} mol dm^{-3}) in the same solvent under an inert atmosphere. After each addition of 0.10 mL, the absorbance was recorded using Hellma optrodes (optical path length 0.1 cm) immersed in the thermostated titration vessel and connected to the spectrometer. Mathematical treatment of the spectrophotometric data was performed with factor analysis[36] and with the SPECFIT program.[30] ^{1}H NMR spectra were recorded at 25 °C on a Bruker Avance 400 MHz. Chemical shifts are given in parts per million with respect to TMS. Diffusion experiments were recorded at 400 MHz proton−Larmor frequency at room temperature. The sequence corresponds to Bruker pulse program *ledbpgp2s*[37] using stimulated echo, bipolar gradients, and longitudinal eddy current delay as the *z* filter. The four 2 ms gradient pulses have sine-bell shapes and amplitudes ranging linearly from 2.5 to 50 G cm^{-1} in 16 steps. The diffusion delay was 100 ms, and the number of scans was 16. The processing was done using a line broadening of 5 Hz, and the diffusion rates were calculated using the Bruker processing package. Pneumatically assisted electrospray (ESI-MS) mass spectra were recorded from 10^{-4} mol dm^{-3} solutions on Finnigan SSQ7000 and Applied Biosystems: MDX SCIEX: API 150 EX instruments. Cyclic voltammograms were recorded using a BAS CV-50W potentiostat connected to a personal computer. A three-electrode system consisting in a stationary Pt disk working electrode, a Pt counter electrode, and a nonaqueous Ag/AgCl reference electrode was used. (^{n}Bu)$_4$NPF$_6$ (0.1 mol dm^{-3} in MeCN) served as an inert electrolyte. The reference potential ($E^0 = -0.16$ V vs SCE) was standardized against [Ru(bipy)$_3$](ClO$_4$)2 (bipy = 2,2′-bipyridyl).[14] The standard scan speed was 100 mV s^{-1}, and voltammograms were analyzed according to established procedures.[14] Elemental analyses were performed by Dr. H. Eder from the Microchemical Laboratory of the University of Geneva, Switzerland.

Conclusion

The reorganization of solvent molecules around the cationic complexes occurring upon Ru(III)/Ru(II)-centered reduction in [RuLn(**L5**)$_3$]$^{(3+z)+}$ or upon complexation of Ln^{3+} to [M(**L5**)$_3$]$^{m+}$ (M = Cr, Ru) is mainly responsible for the apparent lack of considerable intermetallic electrostatic communication in solution and for the surprising stabilities of highly charged self-assembled polymetallic complexes in solution. However, Born−Haber cycles combined with reasonable semiquantitative approximations for estimation of the solvation energies for large cationic complexes restore standard electrostatic trends in the gas phase which can be captured by a simple Coulombic model (i.e., monopole−monopole intermetallic interactions). These results bring some insight into the interpretation of the intermetallic parameters ΔE_{sol}^{MM} fitted by thermodynamic models in solution, which can be now estimated thanks to simple electrostatic calculations in the gas phases "corrected" by solvation energies. It is thus not necessary to invoke either some breakdown of the dielectric continuum (i.e., local dielectric constants)[9] or some drastic polarization of the metallic centers for the rationalization of intercomponent interactions occurring in solution. We are now in a position to eventually reconsider the debatable intermetallic interaction accompanying the successive fixation of Cu(I) in famous Lehn's double-stranded helicates [Cu$_n$(**L8**)$_2$]$^{n+}$ ($n = 1-3$), in which the monovalent cation are separated by 5.8 Å.[1] The use of

(36) Malinowski, E. R.; Howery, D. G. *Factor Analysis in Chemistry*; Wiley: New York, 1980.
(37) Wu, D.; Chen, A.; Johnson, C. S. Jr. *J. Magn. Reson. A* **1995**, *115*, 260−264.

Coulomb eq 4 in the gas phase predicts $\Delta E^{CuCu}_{gas} = 239$ kJ mol^{-1} ($d = 5.8$ Å, $\epsilon_r = 1$), which translates into $\Delta G^0_{K3,gas} - \Delta G^0_{K2,gas} = 121$ kJ mol^{-1} upon application of eq 30 for the successive complexation processes given in equilibria 31 and 32, which strictly mirror those described for $[Eu_n(\mathbf{L3})_3]^{3n+}$ in equilibria 17 and 18 ($n = 1-3$).

$$t\text{-}[Cu(\mathbf{L8})_2]^+ + Cu^+ \rightleftharpoons ct\text{-}[Cu_2(\mathbf{L8})_2]^{2+} \quad \log(K_2) = \log(\beta^{ct}_{22}) - \log(\beta^{t}_{12}) \quad (31)$$

$$ct\text{-}[Cu_2(\mathbf{L8})_2]^{2+} + Cu^+ \rightleftharpoons [Cu_3(\mathbf{L8})_2]^{3+} \quad \log(K_3) = \log(\beta^{tct}_{32}) - \log(\beta^{ct}_{22}) \quad (32)$$

Solvation energies of $\Delta_{solv}G°(t\text{-}[Cu(\mathbf{L8})_2]^+) = -104$ kJ mol^{-1}, $\Delta_{solv}G°(ct\text{-}[Cu_2(\mathbf{L8})_2]^{2+}) = -369$ kJ mol^{-1}, and $\Delta_{solv}G°([Cu_3(\mathbf{L8})_2]^{3+}) = -747$ kJ mol^{-1} can be easily computed with Born eq 6 assuming that (i) $\epsilon_r = 23$ for acetonitrile/dichloromethane (1:1),[2] (ii) $r([Cu_3(\mathbf{L8})_2]^{3+}) = 8.0$ Å in agreement with the experimental spherical hydrodynamic radius in acetonitrile,[23] and (iii) the removal of each Cu(I) on going from $[Cu_3(\mathbf{L8})_3]^{3+}$ to $ct\text{-}[Cu_2(\mathbf{L8})_2]^{2+}$ and finally to $t\text{-}[Cu(\mathbf{L8})_2]^+$ shrinks the cationic radius by stepwise 10% increments, as applied previously for the related $[Eu_3(\mathbf{L3})_3]^{9+}$ system (i.e., $r([ct\text{-}Cu_2(\mathbf{L8})_2]^{2+}) = 7.2$ Å and $r([t\text{-}Cu(\mathbf{L8})_2]^+) = 6.4$ Å). The introduction of these data into eq 24 gives $\Delta G^0_{K3,sol} - \Delta G^0_{K2,sol} = 8$ kJ mol^{-1}, which eventually translates into $\Delta E^{CuCu}_{sol} = 12$ kJ mol^{-1} with eq 30. The latter estimation is in good agreement with $\Delta E^{CuCu}_{exp,sol} = 7$ kJ mol^{-1} extracted from the analysis of the thermodynamic data collected in solution.[5b] Finally, it is worth noting that the same reasoning with a stepwise contraction of only 5% on going from $r([Cu_3(\mathbf{L8})_2]^{3+}) = 8.0$ Å to $r(ct\text{-}[Cu_2(\mathbf{L8})_2]^{2+}) = 7.6$ Å and $r(t\text{-}[Cu(\mathbf{L8})_2]^+) = 7.2$ Å would eventually provide $\Delta E^{CuCu}_{sol} = -43.4$ kJ mol^{-1}, which indeed corresponds to an apparent attraction between Cu(I) cations upon their successive fixation within the double-stranded mold in solution. It is thus not completely absurd to obtain negative intermetallic interaction parameters $\Delta E^{MM}_{exp,sol} < 0$ when the multicomponent assemblies of charged species are analyzed with standard thermodynamic models. We are currently working on the concept of cooperativity associated with these intercomponent parameters because of the dependence on solvation energies.

Acknowledgment. We thank Prof. M. Borkovec for fruitful discussions on solvation energies and Dr P.-Y. Morgantini for constructing Connolly surfaces. Financial support from the Swiss National Science Foundation is gratefully acknowledged.

Supporting Information Available: Figures S1 shows the crystal structures of the cations $[Ru(bipy)_3]^{2+}$ and $[RuLu(\mathbf{L5})_3]^{5+}$ with Connolly surfaces. This material is available free of charge via the Internet at http://pubs.acs.org.

IC062126O